# Liquid Crystalline Polymers in Nematic Solvents: Confinement and Field Effects

**D. R. M. Williams* and A. Halperin***

*Department of Materials, University of California, Santa Barbara, California 93106*

*Received August 20, 1992; Revised Manuscript Received December 30, 1992*

ABSTRACT: The confinement of liquid crystalline polymers dissolved in nematic solvents is analyzed using a mean field theory. For homeotropic boundary conditions the confinement is associated with a tilting phase transition reminescent of the Frederiks transition. When a confined layer is subjected to a suitable magnetic field, reentrant phase behavior is predicted. A partial repression of the tilting transition is expected when the orientation of the field is appropriately changed.

## I. Introduction

The study of liquid crystalline polymers (LCPs) tends to focus on two subjects: the melt state of thermotropic LCPs and the behavior of lyotropic LCPs in isotropic solvents.[1] While thermotropic LCPs are known to be soluble in appropriately chosen nematic solvents,[2,3] little is known of the properties of these solutions. In the following we consider the *confinement behavior* of such solutions[4] with particular attention to the combination of confinement and *electric or magnetic fields*. We focus on solutions of main-chain LCPs consisting of mesogenic monomers joined by flexible spacer chains. For simplicity we consider Θ nematic solvents in which the LCPs retain their melt configurations. The confinement behavior of polymer solutions is a classical and much studied problem in polymer science.[5-9] However, for this novel system qualitatively new features are predicted. These result from the coupling between the orientational order of the nematic medium and the configurations of the LCP. This has two important consequences: (i) The configurations of LCPs in nematic media are anisotropic. (ii) The alignment of a nematic solvent results in the alignment of the LCPs. Thus, if we envision an LCP as an ellipsoid, it is possible to align it with its long axis parallel or perpendicular to the median of the confining slit. As a result, chain *tilt* becomes important as a way to relieve the deformation caused by the confinement. Furthermore, the onset of the tilt can involve a *phase transition*.[4] It should be emphasized that the effect depends essentially on the nematic solvent. It allows us to confine the LCP and, independently, to maintain the alignment of the nematic field at the boundaries. This is not possible for melts of LCP or for lyotropic solutions. Neither of the above-mentioned features has a counterpart in the confinement behavior of homopolymers in isotropic solvents. However, a related effect, the Frederiks transition, is known for single-component nematics.[10] This second-order transition occurs in "single crystal" layers which are well aligned because of the boundary conditions set by the confining surfaces. It is driven by an electric or magnetic field favoring an orthogonal alignment. When the field strength increases beyond a certain critical value, the nematic field is distorted: The bulk attempts to align with the field while the boundary layers are aligned by the bounding surfaces. However, the familiar Frederiks transition is driven only by external fields, and it cannot by triggered by geometrical confinement. Solutions of LCPs in nematic solvents can undergo both the conventional Frederiks phase transition and the confinement-driven transition. When the two effects are combined, other novel scenarios result: The critical field can be made arbitrarily small when the layer approaches the threshold of the confinement-induced transition. Consequently, the phase diagram of the system, in the "thickness-field strength" plane, can exhibit reentrant behavior.

Our mean field analysis combines the continuum theory of nematic liquid crystals with theoretical models for the configurations of LCPs. For convenience we first review the relevant background material on both subjects. Section II contains a brief summary of the continuum theory of nematics[10] illustrated by the analysis of the Frederiks transition in the "bend" geometry. This example is strongly related to the analysis of the confinement behavior. The configurations of LCPs are discussed in section III. It is mostly concerned with thermotropic systems, following the ideas of de Gennes[11a] and of Warner and co-workers.[11b-e] Special attention is given to "hairpin defects".[11] Section IV is devoted to the confinement behavior of solution of main-chain LCP in nematic solvents. The effect of electric or magnetic fields is analyzed in section V. The discussion is devoted primarily to issues of importance to experiments: the solubility of LCPs in nematic solvents and the applicability of "mica machines" to our system.

## II. Continuum Theory and the Frederiks Transition—A Reminder

Our discussion[10] is concerned with uniaxial nematic liquid crystals: At every point, **r**, there is a single preferred direction of molecular orientation. The state of the system is thus specified once we know the tensor $n_{ab} \equiv n_a n_b - {}^1/_3\delta ab$, where **n** is a unit vector, the director, oriented with the locally preferred direction. In this paper we never need to use the full tensor character of the field and we can describe everything satisfactorily using **n**(**r**). The lowest free-energy state corresponds to a perfectly aligned "single-crystal" sample. Phenomenological continuum theory can describe distortions characterized by slow spatial variation on a molecular scale, $a|\nabla \mathbf{n}| \ll 1$, where $a$ is a typical molecular dimension. The excess free-energy density due to the distortion, $f_{dis}$, is obtained by expanding the free-energy density, $f$, in powers of the derivatives of **n**(**r**). The total excess free energy of the system is then $F_{dis} = \int f_{dis} dV$. The expansion, to lowest nonvanishing order in the distortions, is

$$f_{dis} = {}^1/_2K_1(\text{div } \mathbf{n})^2 + {}^1/_2K_2(\mathbf{n}\cdot\text{curl } \mathbf{n})^2 + {}^1/_2K_3(\mathbf{n} \times \text{curl } \mathbf{n})^2 \quad (1)$$

The distortion of the director field is thus associated with a "Hookean" restoring force. The three terms correspond to three types of distortions known, respectively, as splay, twist, and bend. $K_1$, $K_2$, and $K_3$ are the associated elastic

0024-9297/93/2226-2025$04.00/0 

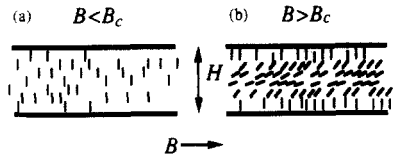


**Figure 1.** Bend geometry for a pure nematic liquid. The director is homeotropically anchored, i.e., perpendicular to the surface. A magnetic field is applied parallel to the surface. (a) For the case of a weak field $\mathcal{B} < \mathcal{B}_c$ the mesogens align perpendicular to the surface throughout the bulk. (b) For the case of a strong field $\mathcal{B} > \mathcal{B}_c$ the system undergoes a Frederiks transition and the director field becomes distorted.

constants. All three are of order $K_i \approx 1 \times 10^{-6}$ dyn. A useful simplification of (1) involves the "one-constant approximation", i.e., $K_1 = K_2 = K_3 = K$.

Distortions of a strongly ordered nematic medium occur as a result of conflicting constraints on the orientation of **n**. The two common constraints are alignment by boundary surfaces, "anchoring", and by electric or magnetic fields, denoted, respectively, by $\mathcal{E}$ and $\mathcal{B}$. The field-induced alignment is due to the anisotropy of the magnetic susceptibility, $\chi$, and the dielectric constants, $\epsilon$, of the nematogens. These constants have different values when measured parallel to **n** ($\chi_\parallel$, $\epsilon_\parallel$) and perpendicular to **n** ($\chi_\perp$, $\epsilon_\perp$). When $\epsilon_\parallel - \epsilon_\perp > 0$ (<0) or $\chi_\parallel - \chi_\perp > 0$ (<0), the applied field favors parallel (perpendicular) alignment of **n** and the field. Anchoring is the imposed orientation of the director at an interface.[12] For example, appropriately treated glass surfaces impose homeotropic (**n** perpendicular to the surface) or homogeneous (**n** parallel to the surface) alignment. Our discussion is mostly concerned with these two situations.

The implementation of the continuum theory is well illustrated by the analysis of the Frederiks transition. This is a second-order phase transition which occurs in thin nematic cells when the orientation imposed by the boundaries conflicts with the alignment favored by the external field, in particular, when the applied electric or magnetic field is perpendicular to the unperturbed **n** as set by the boundary anchoring. This example is of special interest since the confinement behavior of LC polymers involves a similar phase transition. The Frederiks transition can take place in a number of different geometries defined by the choice of surface anchoring and field orientation. The bend geometry (Figure 1), which obtains for homeotropic anchoring, is the most relevant to our case. Consider a thin nematic layer of thickness $H$ confined by two parallel surfaces imposing homeotropic anchoring. The $z$ axis is chosen along the surface normal so that the two boundaries are located at $z = 0$ and $z = H$. In the absence of an external field the unperturbed director field is specified by $\mathbf{n} = (0, 0, 1)$. For specificity we consider the effect of a magnetic field, $\mathcal{B}$, oriented along the $x$ axis, on a nematic with $\Delta\chi = \chi_\parallel - \chi_\perp > 0$. For sufficiently weak fields there is no change in the director field (Figure 1a). However, for $\mathcal{B}$ strong than a certain critical $\mathcal{B}_c$, a new nontrivial solution appears (Figure 1b). The form of the distorted director field is

$$\mathbf{n} = (\sin\theta(z), 0, \cos\theta(z)) \tag{2}$$

where $\theta(z)$, the angle between the director and the $z$ axis must satisfy $\theta(0) = \theta(H) = 0$.

Upon substitution in (1) we obtain

$$f_{dis} = {}^1/_2(K_1 \sin^2\theta + K_3 \cos^2\theta)\theta_z^2 \tag{3}$$

where $\theta_z = d\theta/dz$. The coupling of the nematic director and the magnetic field gives rise to a second, magnetic, contribution to the free-energy density, $f_M$. Since the magnetization is $M = \chi_\perp \mathcal{B} + \Delta\chi(\mathcal{B}\cdot\mathbf{n})\mathbf{n}$, $f_M = M\cdot\mathcal{B}$ is $f_M = -{}^1/_2\Delta\chi(\mathbf{n}\cdot\mathcal{B})^2$, where terms with no **n** dependence are omitted. The resulting total free energy per unit area is

$$F = {}^1/_2\int_0^H dz[(K_1 \sin^2\theta + K_3 \cos^2\theta)\theta_z^2 - (\mathcal{B}^2\Delta\chi)\sin^2\theta] \tag{4}$$

$\theta(z)$ is determined by the Euler–Lagrance equation, $df/d\theta - d(df/d\theta_z)/dz = 0$ or $(K_3 \cos^2\theta + K_1 \sin^2\theta)\theta_{zz} + (K1 - K_3)\theta_z^2 \sin\theta\cos\theta + (\mathcal{B}^2\Delta\chi)\sin\theta\cos\theta = 0$. Just above the critical field, $\mathcal{B}_c$, when $\theta$ is small, this equation may be linearized, yielding

$$K_3\theta_{zz} = -(\mathcal{B}^2\Delta\chi)\theta \tag{5}$$

The solution, allowing for the boundary conditions, is

$$\theta = Q \sin[(\mathcal{B}/\mathcal{B}_c)(\pi z/H)] \tag{6}$$

where

$$\mathcal{B}_c = (\pi/H)(K_3/\Delta\chi)^{1/2} \tag{7}$$

The solution (eq 6) of the linearized eq 5 is valid only when the critical field is applied, so $\mathcal{B} = \mathcal{B}_c$. The linearized equation also supports the trivial solutions $\theta(z) = 0$. A complete solution for $\theta(z)$ is obtained by integration of (5) after it is multiplied by $\theta_z$. The details of this calculation are not important for our purposes. The linearized solution is important for two reasons. First, it allows an exact calculation of the critical field, and second, the first Fourier coefficient of the solution

$$\theta = Q \sin(\pi z/H) \tag{8}$$

is essentially exact for $\mathcal{B} > \mathcal{B}_c$ provided $\mathcal{B}$ is not too large. When $\mathcal{B} \gg \mathcal{B}_c$, the true $\theta(z)$ exhibits a region of low curvature around $z = H/2$, which is not recovered by this approximation.

## III. LC Polymers in Melts and Nematic Solvents

LC polymers in a nematic medium experience an anisotropic molecular field. For thermotropic nematics it is thought that the field is due to a combination of van der Waals attractions and steric, hard core, repulsive interactions. A successful phenomenological description of this field is provided by the Maier–Saupe potential:[11a,c] A unit length of the chain is subject to a field $V(\theta) = a_n - SP_2(\cos\theta)$, where $a_n$ is a coupling constant with units of energy/length, $S = \langle P_2(\cos\theta)\rangle$ is the nematic order parameter, $P_2(\cos\theta)$ is a Legendre polynomial of the second order, and $\theta$ is the angle between the tangent to the chain and **n**. The nematic field affects both the configurations and the spatial orientations of the chains; i.e., the configurations of LCP in nematic media are anisotropic, and the long axis of the molecule has a definite orientation in space. The precise effect depends on the rigidity of the chain, $\epsilon$, its length, $L$, and the temperature, $T$. For rigid, rodlike polymers the effect is purely orientational. The rods tend to align with the director. This case is obtained for chains much shorter than the persistence length $\zeta = \epsilon/kT$. For longer chains it is necessary to allow for the undulations of the semiflexible polymer within a virtual tube due to the nematic field. When the chain length is even longer, $L \gg \lambda = (\epsilon/3a_nS)^{1/2}$, it can support "hairpins", that is, abrupt reversals in the direction of the chain. These impart to the chain the behavior of a one-dimensional random walk in the direction of **n**. Before we introduce the formal description of the system, it is helpful to establish the relevant length scales by using scaling arguments. This part of our discussion is based, with certain modifications, on the presentation of Odijk.[13] We

first consider two reference cases: a rigid rod in a nematic field and a persistent chain in an isotropic medium.

A rigid rod experiences a nematic potential $V(\theta) = Sa_nL \sin^2\theta$, where terms with no $\theta$ dependence were omitted. For strong nematic fields the alignment is strong, $\theta \ll 1$, and the probability density of orientations with a certain $\theta$ is

$$P(\theta) \sim \exp(-Sa_nL\theta^2/kT) \tag{9}$$

$P(\theta)$ is significant when the exponent is of order unity or

$$\langle\theta^2\rangle \approx kT/Sa_nL \tag{10}$$

and thus $\langle\theta^2\rangle \sim L^{-1}$. The second reference system, a persistent chain in an isotropic medium, is a snakelike object. It may bend but it cannot be stretched. The angular correlation between tangents to the chain decay as

$$\langle\cos\theta(\delta)\rangle \approx \exp(-\delta/\zeta) \tag{11}$$

where $\theta(\delta)$ is the angle between two tangents separated by a distance $\delta$ along the contour of the chain. Two limits are important for our discussion: For $\delta \ll \zeta$ the correlation is strong, $\theta \ll 1$ and

$$\langle\theta^2\rangle \approx \delta/\zeta \tag{12}$$

In the opposite limit, $\delta \gg \zeta$, the chain may be viewed as a random walk with steps of length $\zeta$. Thus, a chain of length $L$ has the dimensions of a random walk of $L/\zeta$ steps of length $\zeta$ or

$$R^2 \approx (L/\zeta)\zeta^2 \approx L\zeta \tag{13}$$

How is expression 13, obtained for an isotropic medium with $S = 0$, modified in a *nematic* field?

On long-length scales, $\Delta$, the nematic field is expected to determine $\langle\theta^2\rangle$ according to eq 10, i.e., $\langle\theta^2(\Delta)\rangle \approx kT/Sa_n\Delta$. In the opposite limit, of short-length scales, $\delta$, the nematic contribution is not important and $\langle\theta^2\rangle$ is that of a semiflexible chain in an isotropic medium or $\langle\theta^2(\delta)\rangle \approx \delta/\zeta$. The crossover between the two regimes occurs when the two expressions match, $\langle\theta^2(\delta = \lambda)\rangle = \langle\theta^2(\Delta = \lambda)\rangle$, where $\lambda$ is the "deflection length".[11a,13]

$$\lambda \approx (\epsilon/a_nS)^{1/2} \tag{14}$$

Note that $\lambda \ll \zeta$, that is, the angular correlations decay faster in the nematic medium. This is because a chain in a nematic field is confined, in effect, to a virtual conical capillary. Collisions with the "walls" of the capillary deflect the trajectory of the chain toward the center of the capillary. These deflections accelerate the decay of the angular correlations while imposing strong overall alignment. This picture suggests that the chain is strongly stretched with end to end distance along $\mathbf{n}$ of $R_\parallel \approx L$ and with lateral dimensions of $R_\perp \approx \lambda$. As we shall see, the first conclusion is, in certain regimes, correct, while the second is wrong.

To better understand the lateral dimensions of the chain, consider the effect of the nematic field on a chain segment of one persistence length, $\zeta$. Since $\zeta > \lambda$, the behavior of chain segments of this length is dominated by the nematic field. Each is confined, in effect, to a virtual cone such that $\langle\theta_\zeta^2\rangle \approx kT/Sa_n\zeta$. The diameter of the base of the confining cone, $r$, is roughly determined by $\langle\theta_\zeta^2\rangle \approx r^2/\zeta^2$, thus leading to $r^2 \approx (kT/Sa_n)\zeta \approx \epsilon/Sa_n \approx \lambda^2$. Accordingly, the nematic field, while enforcing the alignment of such chain segments with $\mathbf{n}$, does allow for lateral random walk component of step $\lambda$. Consequently, the chain behaves as a two-dimensional random walk in the plane perpendicular to $\mathbf{n}$. The number of steps is the same as in the isotropic case, $L/\zeta$, but the step length is now $\lambda$ rather than $\zeta$.

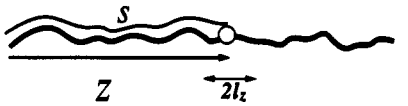


**Figure 2.** Given monomer, indicated here as (○), has both an arc-length position $s$ and an absolute position in real space $z$. $s$ is constant, but because of small thermal wiggles $z$ varies by $\pm l_z$. The size of these variations, $l$, is reminiscent of the de Broglie wavelength of the monomer.

$$R_\perp^2 \approx (L/\zeta)\lambda^2 \tag{15}$$

This defines the small length scale in the problem

$$l \approx \lambda^2/\zeta \approx kT/a_nS \tag{16}$$

$l$ may be thought of as a small elementary step of a random walk component perpendicular to $\mathbf{n}$. For each $\zeta$ segment we have $(\zeta/l)l^2 \approx \lambda^2$ and for the chain as a whole

$$R_\perp^2 \approx (L/l)l^2 = Ll \tag{17}$$

$l$ also has another interpretation as the intrinsic uncertainty in position of a point along the chain (Figure 2). Suppose we are given the arc-length position $s$ of a particular monomer. This does not specify the actual position in space of the monomer, $z$, because small thermal wiggles are continually shifting it back and forth with respect to the end of the chain. Thus, the monomer will be localized about some mean $\bar{z}$ but with a standard deviation $l_z$ and will hence usually be found somewhere within $z \in (z - l_z, z + l_z)$. To find $l_z$, we consider a section of chain of length $\mu > \lambda$. On such a length scale the nematic energy dominates the elastic contribution, and the angle made by the length $\mu$ with the director obeys $\langle\theta^2\rangle \approx kT/(3a_nS\mu)$. As the angle oscillates between 0 and $kT/(3a_nS\mu)$, the projection of the length $\mu$ on the director varies between $\mu$ and $\mu\cos\theta$, and thus $l_z \approx \mu - \mu\cos\theta \approx \mu\langle\theta^2\rangle \approx kT/3aS \approx l$. Since in general $l/\lambda \sim kT/U_h \ll 1$, any point on the chain is localized to within better than a deflection length. The result that $l_z \approx l$ was obtained by Gunn and Warner[11b] using a more complicated and exact analysis. It is important to distinguish $l$ from $\lambda$ especially when using the ideal gas model for hairpins described below.

At this point we can introduce a more formal approach to the problem, based on the energy functional, $U$, of a persistent chain in a nematic field.[11] For long chains, $L > \zeta$, $U$ consists of two terms:

$$U = \frac{3}{2}a_nS\int_0^L \sin^2\theta ds + \frac{\epsilon}{2}\int_0^L \left(\frac{d\theta}{ds}\right)^2 ds \tag{18}$$

The first reflects the effect of the nematic field allowing for the local orientation of the chain. The bending energy of the semiflexible chain gives rise to the second term. The reader should note that this energy functional is valid for a melt of chains. In a nematic solvent it will be renormalized. In what follows we neglect this renormalization. Our discussion thus far, of a strongly stretched chain with small undulations, corresponds to the linearized version of (18):

$$U = \frac{3}{2}a_nS\int_0^L \theta^2 ds + \frac{\epsilon}{2}\int_0^L \left(\frac{d\theta}{ds}\right)^2 ds \tag{19}$$

The deflection length, $\lambda$, appears now in two related roles. First, it is the healing length determining the size of the distorted region of a chain subject to a perturbation of its orientation. This is easily seen from the linearized Euler–Lagrange equation corresponding to (18), $\lambda^2 d^2\theta/ds^2 = \theta$, which specifies the equilibrium configuration of the con-

strained chain. When $0 < \theta(0) \ll 1$ and $\theta(L) \to 0$ as $L \to \infty$, this equation is solved by $\theta = \theta(0)\exp(-s/\lambda)$. The linearized $U$ also suggests an Ornstein–Zernicke analysis of the shape fluctuations.[13] In this context $\lambda$ assumes its second role as the correlation length characterizing the decay of the fluctuations. $\theta(s)$ is expanded as Fourier series in the length $L$, $\theta = \sum_q \theta_q \exp(iqs)$, where $\theta_{-q} = \theta_q^*$ since $\theta$ is real. Substitution in (19) yields $U = L\sum_q (3a_nS/2 + \epsilon q^2/2)|\theta_q|^2$. The equipartition theorem assigns an average energy of $kT$ to each mode. Accordingly, the average amplitude of the $q$ mode is

$$\langle|\theta_q|^2\rangle = kT/L(3a_nS/2 + \epsilon q^2/2) = (2kT/L\epsilon)(\lambda^{-2} + q^2)^{-1} \tag{20}$$

and the corresponding correlation function is

$$\langle\theta(s)\theta(s + \Delta s)\rangle = \frac{1}{2\pi}\frac{\zeta}{\Delta s}\exp(-\Delta s/\lambda) \tag{21}$$

One should note that the modes considered above do not correspond to states of mechanical equilibrium. Such states are specified by stationary solutions for $U$ which satisfy the Euler–Lagrance equation $\lambda^2 d^2\theta/ds^2 = \theta$. For polymers with free ends the solutions must also satisfy the boundary conditions $d\theta/ds = 0$ at both ends. Thus, the only mechanical equilibrium state consistent with eq 19 is a straight line. In marked distinction, the nonlinearized $U$ does allow for nontrivial states of mechanical equilibrium.[11] The corresponding Euler–Lagrange equation is

$$\lambda^2 d^2\theta/ds^2 = \sin\theta\cos\theta \tag{22}$$

For an infinitely long chain the nontrivial solution is

$$\cos\theta = \tanh s/\lambda \tag{23}$$

and the associated energy, of order $\epsilon/\lambda$, is

$$U_h = 2(3a_nS\epsilon)^{1/2} \tag{24}$$

Similar but more complicated solutions are found for finite yet long chains.[11d] For convenience we mostly neglect these finite size effects. Equation 23 describes a "hairpin" defect in the chain, i.e., a rapid reversal in the direction of the chain. A single hairpin is comprised of two arms which are aligned with **n** and joined by a bend. The size of the bend, a few $\lambda$'s, represents a balance between the elastic penalty, which favors gradual bend, and the nematic contribution, which promotes an abrupt change of direction so as to maximize the alignment with the nematic field. A more detailed analysis, allowing for finite size effects, suggests that a chain of length $L$ can support up to $\approx L/\lambda$ hairpins in mechanical equilibrium.[11d] Because of their marginal stability, hairpins are expected to be long-lived and may be treated as quasiparticles. Accordingly, $n$ hairpin defects on a chain of length $L$ may be viewed as a one-dimensional solution of $n$ particles, with localization length $l$, in a length $L$. The corresponding free energy is

$$F = nU_h + nkT\ln(nl/L) \tag{25}$$

where $nl/L$ is the length fraction of the quasiparticles. $\lambda$, the particle "size", plays no role in the thermodynamics because of the absence of excluded volume interactions between the hairpins. $l$, which is reminiescent of the de Broglie wavelength, defines an effective lattice constant which allows for the uncertainty in the position of the hairpin. Actually, there are two kinds of interactions between the hairpins. The first are short-ranged attractions, propagated along the chain backbone, of the form $\exp(-\delta/\lambda)$, where $\delta$ is the distance between the two hairpins. The second type is mediated by the nematic environment.[11] These interactions are irrelevant, providing the concentration of hairpins is low enough. Minimization of $F$ with respect to $n$ yields the average equilibrium number of hairpins, $\langle n\rangle$, on a chain characterized by $L$, $U_h$, and $T$

$$\langle n\rangle = (L/l)\exp(-U_h/kT) \tag{26}$$

When $\langle n\rangle \gg 1$, the chain performs a one-dimensional random walk in the direction of **n**. The number of steps is $\langle n\rangle$, and the average step length is $L/\langle n\rangle$. Accordingly, the average size of the chain parallel to **n** is

$$R_\parallel^2 \approx L^2/\langle n\rangle = Ll\exp(U_h/kT) \tag{27}$$

and thus $\langle R_\parallel^2\rangle/\langle R_\parallel^2\rangle = \exp(U_h/kT)$. The reader should bear in mind that any renormalization of the Hamiltonian has large (exponential) consequences for $R_\parallel^2$.

Our discussion thus far dealt with thermotropic LCP in nematic media following the ideas of de Gennes and of Warner and co-workers. Two situations are possible: a melt of LCPs or a solution of LCPs in a nematic solvent of low molecular weight. In the second case the discussion neglects excluded volume effects. In both systems the nematic field is modeled by mean field Maier–Saupe interaction. Similar ideas were developed for lyotropic solutions of semiflexible LCPs in isotropic solvents. In such systems it is often assumed that the dominant interactions are hard core steric repulsions. This direction was pursued by Khokhlov and Semenov[14] and by Odijk.[13] Lyotropic solutions are not expected to exhibit the confinement behavior of LCPs in nematic solvents since it is impossible to align the isotropic solvent. Nevertheless, for completeness, it is of interest to briefly review the theoretical description of lyotropic systems.

The behavior of the two systems is in many respects similar. The main difference is in the nature of the control parameter for the phase behavior. In thermotropic systems it is temperature, while for lyotropic solutions it is the concentration. Thus, if the probability density for a given $\theta$ in a lyotropic solution is assumed to be Gaussian

$$P(\theta) \sim \exp(-\alpha\theta^2) \tag{28}$$

one finds $\lambda \approx \zeta/\alpha$, etc., along the lines described earlier. However in the lyotropic case $\alpha$ is a function of concentration. It is found by minimizing the appropriate free energy. This is comprised of two important terms: One, $F_c$, allows for the deformation of the chain by the nematic field by assigning $kT$ to each deflection. The confinement free energy of a rod of length $L$ in a capillary of diameter $D$ is roughly $-kT\ln(D/L)^2$. Viewing the semiflexible chain as a succession of confined rods of length $\lambda$, we obtain $kT(L/\lambda)\ln(L/\lambda) \approx kTL/\lambda$. For a solution of $N$ chains we thus have $F_c/kT \approx N(L/\lambda)$. The second term, $F_{ex}$, accounts for Onsager-type excluded volume interactions. This may be approximated as $F_{ex}/kT \approx (N^2L^2/V\lambda^2)b\rho$, where $b \approx \lambda^2 D$ is the average excluded volume of chain segments of length $\lambda$ and diameter $D$. $\rho \approx \alpha^{-1/2}$ is the average angle between the rods, and the term in parentheses is $Vc^2$, where $c = NL/\lambda V$ is the concentration of persistent segments in a volume $V$. Minimization of $F = F_{ex} + F_c$ with respect to $\alpha$ leads to

$$\alpha \sim (\zeta/D)^{2/3}\phi^{2/3} \tag{29}$$

where $\phi \approx LD^2/V$ is the volume fraction of LCP. Using more elaborate arguments, it is possible to produce an Ornstein–Zernicke analysis of the small undulations. The discussion of hairpins is somewhat more problematical. If one postulates their existence and an associated energy

penalty of $\epsilon/\lambda$, it is possible to use (25) to obtain $\langle n \rangle$ and $R_\parallel^2$. This route was taken by Vroege and Odijk[15] (their eq II.4), who mistakenly identified the localization length $l_z$ with $\lambda$, whereas in fact it is $l \ll \lambda$ (see also ref 11m, where it is also claimed that there is only one length and hence $\lambda = l_z$). On the other hand, the implementation of a rigorous theory is more complicated. For lyotropic LCPs of long length $L \gg \zeta$, the polymer may be envisioned as a semiflexible chain comprised of rods of length $\zeta$. In turn, the rods experience only infinitely strong steric repulsions. Accordingly, it makes little sense to talk of the energy functional of the chain $U$. As a result, the properties of hairpins cannot be deduced from $U$. Rather, one must proceed directly to the free energy, $F$. This is written in a way which is analogous to the Onsager theory for hard rods. There are two terms: first, an entropic term which favors random directions for the chain segments, and second, a virial term due to the interactions between pairs of segments of length $l_s$. This term favors alignment of the chain segments. $F$ is expresses in terms of an orientational distribution function for the chain segments, $f(\Omega)$, and the concentration of effective segments, $c$.[14]

$$F/(kT) = N\int \frac{d\Omega}{4\pi} \frac{[\nabla_\Omega f(\Omega)]^2}{4f(\Omega)} + \frac{1}{2}Nc\int \frac{d\Omega}{4\pi}\frac{d\Omega'}{4\pi} f(\Omega)f(\Omega')B(\Omega,\Omega') \quad (30)$$

where $B(\Omega,\Omega')$ is the second virial coefficient between two rods of length $l_s$ pointing in directions $\Omega$ and $\Omega'$. Using this $F$, Khokhlov and Semenov[16] have been able to calculate the response of a persistent chain to a dipolar, $P_1(\cos\theta)$, field (such as an electric field or an extensional force) acting along the director. In the limit of vanishingly small fields they calculate the susceptibility which is related to the chain dimensions by $\chi_0 = \langle R_\parallel^2 \rangle_0/(l_s L)$. In turn $\chi_0$ determines the parallel extent of the chain and hence the number of hairpins. Vroege and Odijk[15] reanalyzed the problem and obtained somewhat different results. One of their expressions, (VIII.15), agrees with eq 27. There is thus some general agreement between the Maier–Saupe approach in melts and the Onsager approach in solvents. The details of these studies are, however, beyond the scope of our discussion.

## IV. Polymer Solution between Plates

In this section we study the confinement behavior of main-chain LCPs in a nematic solvent.[4] The low molecular weight nematic is assumed to be a Θ solvent in the sense that the configurations of the LCP are those found in a melt. This assumption simplifies the analysis but is not crucial for the effect. Similar phenomenology is expected in good solvents. The nematic solvent considered is strongly ordered; i.e., it is well below the clearing temperature. The LCP solution is taken to be semidilute; that is, the LCP concentration is above the overlap threshold of the chains. This allows us to assume lateral uniformity in the confined layer. The LCPs are assumed to be long enough so that each chain supports many hairpins, $\langle n \rangle \gg 1$. We further assume that the LCPs, or more precisely the arms of the hairpins, follow, on average, the nematic director. This assumption is justified provided the director varies slowly enough: $\lambda|\nabla \mathbf{n}| \ll 1$. The solution is confined between two flat surfaces such that the distance between the plates is $H$. The confined solution is not coupled to any reservoir. As a result, the number of chains per unit volume is constant.

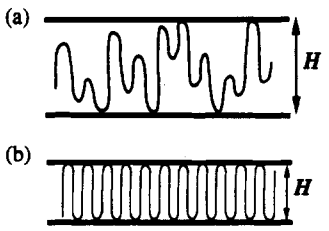


**Figure 3.** (a) Single chain undergoing weak confinement between two plates. In this regime the confining force is Gaussian and the hairpins are rearranged to fit between the plates. (b) Strongly confined chain. The distance between the plates is less than the interhairpin distance in an unconfined chain, and the chain must form extra hairpins. In this regime the free energy is dominated by the energy of the extra hairpins.

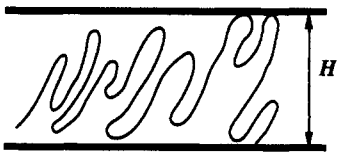


**Figure 4.** Tilted chain. By tilting, the chain increases the arc-length it uses in going between the plates. This lowers the confinement free energy.

Different confinement behavior is expected for different anchoring conditions. When the plates impose homogeneous boundary conditions, the resulting scenario is standard. For $H > \langle R_\perp \rangle$ the LCPs are essentially free, while a Gaussian confinement behavior is expected for $H < \langle R_\perp \rangle$. In particular, the elastic free energy per chain is $f_c/kT \approx (\langle R_\perp \rangle/H)^2$. A richer behavior is expected in the case of homeotropic alignment. When the possibility of nematic distortion is ignored, it is possible to envision three important regimes: For large plate separations, much greater than the parallel radius of gyration of the chains $\langle R_\parallel \rangle$, the chains are essentially unconfined and the plates have no effect. When $H < \langle R_\parallel \rangle$, the chains are confined and the system pays an energy penalty for this confinement. For weak confinement the elastic free energy penalty per chain must be Gaussian and so has the form

$$f_{el} \approx kT(\langle R_\parallel \rangle/H)^2 \quad (31)$$

In this regime (Figure 3a), $\langle n \rangle$ is determined approximately by (26) and the confinement causes spatial rearrangement of the hairpins. At larger compressions we enter a "hairpin creation" regime. Two such regimes are conceivable. In one scenario hairpins are created to relieve the Gaussian penalty. This is expected for $H$ such that $f_{el} \approx U_h$. Another scenario occurs when the condition $H \sim L/\langle n \rangle$ is obtained before $f_{el} \approx U_h$ (Figure 3b). In this case the average spacing between hairpins, assuming "ground-state dominance", is $H$ and the dominant term in the free energy is $F = U_h L/H$, where $L/H$ is the number of hairpins. In both hairpin creation regimes the number of hairpins is a function of $H$ rather than $T$.

The three regimes of the homeotropic confinement are obtained if the chains remain perpendicular to the plates. However, chain tilt can relieve the deformation penalty (Figure 4). The benefits are easily seen if we assume that the chains are tilted with a constant angle, $\theta$. In this oversimplified picture the Gaussian penalty is reduced from $kT(R_\parallel/H)^2$ to $kT(R_\parallel/H)^2\cos^2\theta$. In the hairpin creation regime the penalty is reduced from $(L/H)U_h$ to $(L/H)U_h \cos\theta$ since the hairpin arms can now be longer. This simple-minded argument focuses on the LCPs while ignoring the nematic solvent. However, the two are strongly coupled because of our assumption that the chains locally follow the director. Since the nematic solvent must obey the homeotropic boundary conditions, it is necessary to allow

for the distortion of the nematic field. As a result, the constant tilt is replaced by a height-dependent tilt. As we shall see, the development of the tilt involves a phase transition reminescent of the Frederiks transition in the "bend" geometry. However, in our case the transition is due to the confinement of the LCP rather than the application of an external field. Our aim here is to predict the phase diagram for this system and delimit the tilted and untilted regions. To proceed, we need the free energy per unit area of the confined layer, $F$. This consists of two terms. One allows for the distortion free energy of the nematic and the second for the deformation of the LCP. Both terms are determined by the angle made by the director at a height $z$ above the lower plate. This angle, as measured with respect to the plate normal, we call $\theta(z)$. Because the solvent is homeotropically anchored, it satisfies $\theta(0) = \theta(H) = 0$. Within the one-constant approximation the nematic solvent distortion term for a layer of area $\Sigma$ is

$$F_{dis} = \Sigma(1-\phi)(K/2)\int_0^H dz(d\theta/dz)^2 \quad (32)$$

where $K$ ia an elastic constant of the nematic and $\phi$ is the volume fraction of chains. If $a$ is a typical chain monomer size and $L$ is the chain length, then the number of chains in our section of area $\Sigma$ is $\Sigma H\phi/a^2L$. The chain elasticity contribution to the free energy is then[17]

$$F_{el} = kT(\Sigma H\phi/a^2L)[(R_\parallel/\rho)^2 + \ln(\rho/R_\parallel)^2] \quad (33)$$

where $\rho$ is the arc-length distance followed by the polymer in traversing the distance between the plates

$$\rho = \int_0^H [dz/\cos\theta(z)] \quad (34)$$

It is through $\rho$ that the director distortion $\theta(z)$ enters into the chain free energy. $F_{el}$ is given by the full Gaussian elastic penalty. In this case the second term is crucial to the analysis since in its absence there would be no transition. We return to this below. Also, the reader should keep in mind that while our results include the limit $H \to 0$, this limit is beyond the region of validity of the theory.

The free energy considered above, $F_{dis} + F_{el}$, is based on two approximations. First, we ignore, at this stage, possible contribution due to the bending elasticity of the chain. That is, it is assumed that the chain is not penalized for following the director. We investigate this issue in detail later on. Also, we ignore the coupling of the LCP concentration profile and the director field. In particular, no allowance is made for the possibility of an LCP depletion layer at the boundary, where the director field does not favor tilted configurations. This assumption is justified for weak tilts, at the vicinity of the transition. Finally, it is helpful to note the similarity between this case and the Frederiks transition reviewed in section II: The distortion term is identical in the two cases. As we shall see, so is $\theta(z)$, at least near the transition. On the other hand, the magnetic (electric) term, $F_M$, is replaced by $F_{el}$. Also, in the present case each term refers to a different component, thus giving rise to the $\phi$ dependence. The discussion of the normal Frederiks transition involves a single-component system and the two terms reflect different interactions of this component.

To analyze the phase behavior, we will use a trial function for $\theta(z)$

$$\theta(z) = Q\sin(\pi z/H) \quad (35)$$

This trial function is suggested by the analysis of the Frederiks transition. In this case as well it can be shown

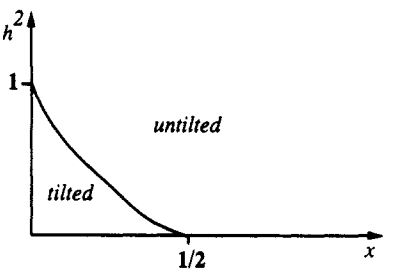


**Figure 5.** Phase diagram for the tilting transition in the case where chain rigidity is of negligible importance, $\kappa \ll 1$. $h$ is the scaled separation between the plates, and $x$ measures the relative importance of the nematic distortion and the chain deformation. The line is a line of second-order phase transitions. For $h > 1$ there is no compression and the chain is untilted. When $h < 1$, the chain tilts to relieve the compression. However, for $x > 1/2$ there is no tilt because the nematic distortion penalty is too high.

to be exact at the vicinity of the transition (Appendix). $Q$ plays the role of the order parameter in our analysis. When $Q = 0$, there is no tilt and the strength of the tilt grows with $Q$. Upon substitution of (35) in (32–34) we can expand $F$ in powers of $Q$. The resulting Landau free energy is

$$F = [(1-\phi)\Sigma K\pi^2/4H]Q^2 + [kT\sigma H\phi/a^2L][R_\parallel^2\rho^{-2} + \ln(\rho^2/R_\parallel^2)] \quad (36)$$

where

$$\rho \approx H[1 + Q^2/4 + 5Q^4/64 + 61Q^6/2304] \quad (37)$$

This $F$ may be rendered dimensionless if multiplied by $[(1-\phi)\Sigma K\pi^2/4H]^{-1}$, yielding

$$F \approx \frac{A}{2}Q^2 + \frac{B}{4}Q^4 + \frac{C}{6}Q^6 + O(Q^8) \quad (38)$$

where $A = (1/x)(h^2 - 1 + 2x)$, $B = (1/8x)(1 + 3h^2)$, and $C = (1/96x)(1 + 14h^2)$. Here we have introduced two dimensionless variables: The first

$$h = H/R_\parallel \quad (39)$$

gives a dimensionless measure of the compression. Only for $h < 1$ is the system compressed, and only in this regime is our free energy meaningful. The second dimensionless parameter is

$$x = (\pi^2/4)(Ka/kT)(La/R_\parallel^2)((1-\phi)/\phi) \quad (40)$$

Roughly speaking $x \approx F_{dis}(Q = 1)/F_{el}(Q = 0)$ measures the relative importance of the nematic distortion and the chain deformation. For large $x$ the distortion of the nematic director is dominant and the system is untilted. For small $x$ the chain distortion term is relatively more important and we expect a tilted phase. The behavior of the system for $x \approx 1$ remains to be determined. This can be deduced by standard analysis of the Landau free energy.[18] We have positive $B$ and $C$ for all physical $x$ and $h$. $A$ can, however, change sign. It may be written as $A = x^{-1}(h^2 - h_c^2)$, where $h_c^2 = 1 - 2x$. This is the signature of a second-order phase transition at $h = h_c$. For $h > h_c$, $F$ has a single minimum at $Q = 0$, while for $h < h_c$, the minimum is shifted to $Q > 0$ given by

$$Q = \frac{-B + (B^2 - 4AC)^{1/2}}{2C} \approx -A/BC \quad (41)$$

Accordingly, the system exhibits a line of second-order phase transitions in the $h^2$ vs $x$ plane (Figure 5) which is

specified by

$$h_c^2 = 1 - 2x \tag{42}$$

The logarithmic term in $F_{el}$ gives rise to the $h$ dependence of $A$ and is thus essential for this effect. When this term is ignored, both $F_{dis}$ and $F_{el}$ scale as $H^{-1}$ and $H$ cannot drive the phase transition.

Our discussion thus far overlooked a possible contribution due to the bending elasticity of the chains. Since the chains are assumed to follow the director, it is necessary to consider an extra term in $F$, $F_{bend}$, given by

$$F_{bend} = \frac{\epsilon}{2}\int_0^L ds\left(\frac{d\theta}{ds}\right)^2 \tag{43}$$

Since the plate to plate distance along the director is $\rho$ as given by (34) and since $ds = dz/\cos\theta$, it is possible to approximate $F_{bend}$ as

$$F_{bend} \approx \frac{L}{\rho}\frac{\epsilon}{2}\int_0^H dz\cos\theta\left(\frac{d\theta}{dz}\right)^2 \tag{44}$$

In terms of our trial function $\theta(z) = Q\sin(\pi z/H)$ we have

$$F_{bend} = \frac{\epsilon}{2}L\left(\frac{\pi}{H}\right)^2 Q^2 \frac{\int_0^\pi du\cos^2 u\cos(Q\sin u)}{\int_0^\pi du\frac{1}{\cos(Q\sin u)}} \approx \frac{\epsilon}{2}L\left(\frac{\pi}{H}\right)^2 Q^2 \frac{\left[\frac{\pi}{2} - \frac{\pi}{16}Q^2 + \frac{\pi}{384}Q^4\right]}{\left[\pi + \frac{\pi}{4}Q^2 + \frac{5\pi}{64}Q^4\right]} \tag{45}$$

Further manipulation yields a dimensionless free energy per unit area of

$$F_{bend} = \frac{\kappa}{x}\left[\frac{1}{2}Q^2 - \frac{3}{16}Q^4 + \frac{1}{96}Q^6\right] \tag{46}$$

where $\kappa$ is a new dimensionless parameter defined by

$$\kappa = \pi^2\epsilon L/2kTR_\parallel^2 \tag{47}$$

$\kappa$ may be interpreted as $\kappa \approx F_{bend}(Q=1)/F_{el}(Q=1)$. It is easily seen that $\kappa \sim \zeta/(L/\langle n\rangle)$; i.e., it is the ratio of the persistence length and the average distance between hairpins. Clearly, when $\kappa \ll 1$, the bending term is of little importance and our earlier analysis is essential correct. In the opposite case, when $\kappa \gg 1$, the bending term is dominant and the analysis must be modified. This is indeed the case. Because of $F_{bend}$ the coefficients of the Landau free energy are modified to $A = (1/x)(h^2 - 1 + 2x + \kappa)$, $B = (1/8x)(1 + 3h^2 - 6\kappa)$, and $C = (1/96x)(1 + 14h^2 + 6\kappa)$. An important new feature is that $B$ as well as $A$ can now change sign. As a result, the system can undergo a first-order phase transition. As expected, for small $\kappa$ the system undergoes a second-order phase transition. The critical $h$ is, however, slightly lower

$$h_c^2 = 1 - 2x - \kappa \tag{48}$$

Thus, while the phase diagram is similar to that depicted in Figure 5, the tilting transition requires greater compression. This is not surprising since tilt increases chain bending and hence $F_{bend}$ opposes tilt. For larger $\kappa$ a qualitatively different behavior is found. The line of second-order phase transitions joins a line of first-order phase transitions at a tricritical point specified by $A = B = 0$ or

$$x_t = \frac{2}{3} - \frac{3}{2}\kappa \tag{49}$$

The first-order transition occurs only for $\kappa > 1/9$ and for $x > x_t$ (Figure 6). However, this first-order phase transition may be difficult to attain. The reason is that $\kappa > 1$ is unlikely in our system: the expressions for $\zeta$ and $\langle n\rangle$ lead to

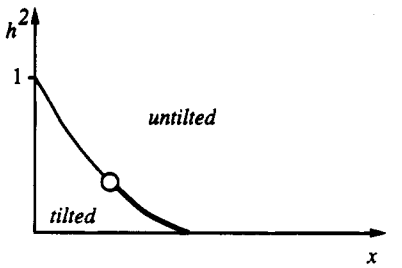


**Figure 6.** Phase diagram when the chain rigidity is important, $\kappa > 1/9$. Again, a tilting transition takes place for strong compression (small $h$), but the transition can be first (thick line) or second (thin line) order. The second- and first-order lines meet at a tricritical point (O). Note, however, that the first-order transition is near the limit of the theoretical model.

$$\kappa \sim (U_h/kT)^2\exp(-U_h/kT) \tag{50}$$

Since we assume that $U_h > kT$, we expect $\kappa < 1$.

Earlier in this section we considered the case where the nematic solvent and the polymer chains tilt simultaneously. It is possible to imagine a situation where the chains tilt but the director for the solvent molecules remains perpendicular to the plates; i.e., the chains do not follow the director. In this case the tilt relieves the deformation of the chain at the price of a nematic energy penalty. The free energy for one chain is thus

$$F = kT[(R_\parallel\cos\theta/H)^2 + \ln(H/R_\parallel\cos\theta)^2] + \frac{3}{2}a_nSL\sin^2\theta \tag{51}$$

where $\theta$ is the tilt angle. If we expand this free energy with respect to $\theta$, we find the possibility of a second-order phase transition for

$$h^2 < (1 + L/l)^{-1} \tag{52}$$

Since $L \gg l$, this requires very strong compression. Since the "simultaneous" tilt transition occurs at weaker confinement, this last scenario is ruled out within this analysis.

## V. Application of a Magnetic Field

As noted above, the confinement-induced tilting phase transition is closely related to the Frederiks transition. The two transitions differ primarily with regard to the nature of the driving force, i.e., confinement-induced deformation of LCP vs. magnetic or electric fields. It is thus of interest to combine the two effects: One may use an electric or magnetic field to drive a tilting transition when the confinement is subcritical. As we shall see, in such cases very weak fields are sufficient. For brevity we only consider the case of a magnetic field aligned in parallel with the surface. We assume, for simplicity, that $\Delta\chi$ ($>0$) values of the solvent and of the polymer are identical. We further focus on the case of $\kappa \ll 1$ when the chain rigidity is irrelevant.

The effect of the field on an unconfined layer was considered in section II. The feature of interest is the $H$ dependence of the critical field

$$\mathcal{B}_c = \frac{\pi}{H}\left(\frac{K}{\Delta\chi}\right)^{1/2} \tag{53}$$

In other words, the critical field needed to induce a Frederiks transition increases as $H^{-1}$ because the distortion penalty of the layer increases as it grows thinner. It is useful to reformulate this result in terms of the magnetic

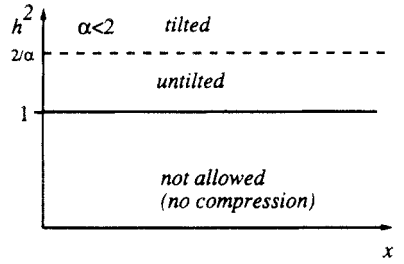


**Figure 7.** Phase diagram for the system in the presence of a small field ($\alpha < 2$) but with no confinement. For a thick layer ($h^2 > 2/\alpha$) the director field is bent to align more with the magnetic field. For a thin layer ($h^2 < 2/\alpha$), the tendency to align to resisted fully by the bulk nematic bending penalty. The second-order line at $h^2 \approx 2/\alpha$ corresponds to the Frederiks transition. The region $h^2 < 1$ is forbidden in this diagram since we are examining the case of no compression.

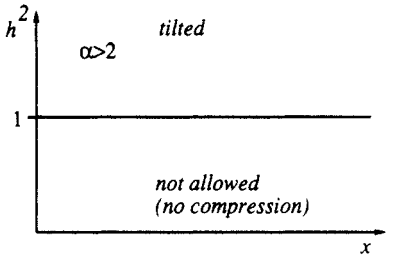


**Figure 8.** Phase diagram in the presence of a large field ($\alpha > 2$) but with no confinement. The whole uncompressed region has undergone a Frederiks transition and is tilted.

coherence length $\xi_B = (K/\Delta\chi)^{1/2}\mathcal{B}^{-1}$.[10] This measures the decay of a perturbation in a sample oriented by a magnetic field of strength $\mathcal{B}$. The Frederiks transition occurs when $\xi_B = H/\pi$. Finally, note that $F_{dis}$ as given by (32) ignores the polymer contribution to the nematic distortion energy. We are thus limiting our analysis here to low polymer volume fraction $\phi \ll 1$.

When $\kappa \ll 1$, the free energy per area $\Sigma$ of the confined layer, $F$, as given by (36), must be supplemented by an extra term, $F_M$, due to the interaction with the magnetic field:

$$F_M = -\frac{1}{2}\Delta\chi\Sigma\mathcal{B}^2\int_0^H dz\, \sin^2(\theta(z)) \qquad (54)$$

By multiplying by $[(1 - \phi)\Sigma K\pi^2/4H]^{-1}$, we find the following dimensionless magnetic free energy

$$F_M = -\alpha h^2\int_0^\pi du\, \sin^2(Q\sin(u)) \approx \alpha h^2\left[-\frac{Q^2}{2} + \frac{Q^4}{8} - \frac{Q^6}{72} + \frac{Q^8}{1152}\right] \qquad (55)$$

where $\alpha = 2\Delta\chi\mathcal{B}^2R_\parallel^2/(\pi^2K(1 - \phi))$ and $\alpha h^2 \approx F_M(Q = 1)/F_{dis}(Q = 1)$. It is instructive to express $\alpha$ in terms of $\xi_B$ leading to $\alpha = (2/(1 - \phi))(R_\parallel^2/\pi^2\xi_B^2)$. Note that the second factor involves the threshold condition for the occurrence of a Frederiks transition in a layer of thickness $R_\parallel$. Before the effect of polymer compression is analyzed, it is useful to draw the phase diagrams for the ordinary Frederiks transition (Figures 7 and 8). The coefficients of the Landau free energy are

$$A = \frac{1}{x}[h^2(1 - \alpha x) - (1 - 2x)] \qquad (56)$$

$$B = \frac{1}{8x}[1 + 3h^2 + 4x\alpha h^2] \qquad (57)$$

$$C = \frac{1}{96x}[1 + 14h^2 - 8x\alpha h^2] \qquad (58)$$

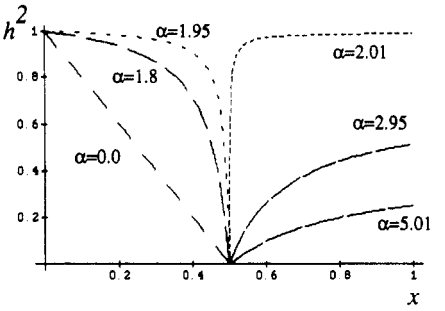


**Figure 9.** Plots of the critical line $h_c^2 = (1 - 2x)/(1 - \alpha x)$ for various values of the field strength $\alpha$. The topology of the diagram changes suddenly at $\alpha = 2$.

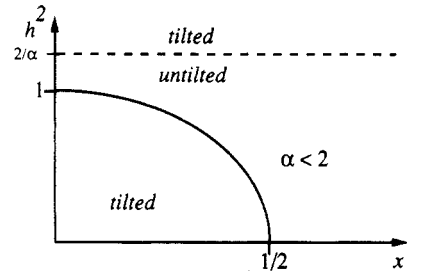


**Figure 10.** Re-entrant phase diagram in the presence of both a weak field ($\alpha < 2$) and comparison. For $h^2 > 2/\alpha$ there is no compression and the system is tilted because of the field. At small $h$ (and for $x < 1/2$) the system is tilted because of compression. In the intermediate regime there is an untilted region. In this region the layer is too thin to be bent by the field, and for $x < 1/2$ it has not be sufficiently compressed to tilt via compression. For $x > 1/2$ both the polymer contribution and the field contribution are insufficient to overcome the bulk nematic penalty giving rise to an untilted region.

The standard analysis of the Landau free energy is easily extended to this case. However, one important limitation must be kept in mind: for strong enough fields $\alpha > (1/8x)(h^{-2} + 14)$ it is possible to have $C < 0$. When $C < 0$, the truncated free-energy expansion corresponds to an unstable system. One may avoid this problem by retaining higher order terms. However, in the following we confine ourselves to sufficiently weak fields, when this problem does not arise. As in the case of simple confinement we find a line of second-order transitions specified by $A = 0$ or

$$h_c^2 = (1 - 2x)/(1 - \alpha x) \qquad (59)$$

This function is plotted in Figure 9 for various values of the field strength $\alpha$. The phase behavior in this case is, however, quite distinctive. Two regimes, depending on the field strength $\mathcal{B}$, can be distinguished. For low fields, such that $\alpha < 2$, a tilted phase can be found, as usual, for $h > \pi\xi_B/R_\parallel$ (Figure 10). The magnetic field also reinforces the confinement contribution in causing tilt for $h < 1$. This results in expansion of the boundaries of the tilted domain for the confined layer, $h < 1$. For intermediate $h$ values the layer remains untilted. Furthermore, no tilt occurs for $x > 1/2$. This reentrant behavior disappears when the field is strong enough to align a layer of thickness $R_\parallel$, i.e., $\alpha = 2$ and $\xi_B \approx \pi/R_\parallel$. For $\alpha > 2$ (Figure 11) the layer is untilted only for low $h$ and $x > 1/2$. In this region the combined effects of the polymer deformation and the magnetic field are too weak to overcome the nematic distortion penalty. The boundaries of the tilted region occur below the $\xi_B \approx \pi/R_\parallel$ line. The layer is tilted for all $h$ provided $\alpha > 2$ and $x < 1/2$.

Another property of interest is the critical field, $\mathcal{B}_c$, and its dependence on the layers thickness, $H$. For low

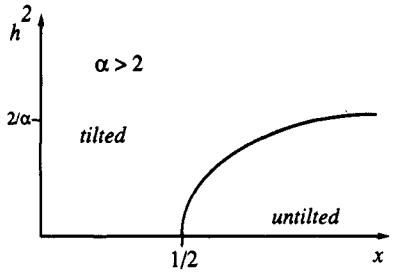


**Figure 11.** Phase diagram for a strong field ($\alpha > 2$) and compression. Tilting predominates, except in a region of large compressions for $x > 1/2$. Here both the magnetic field and the polymer compression favor tilting. However, for $x > 1/2$ and small $h$ the nematic distortion, which opposes tilting, is dominant.

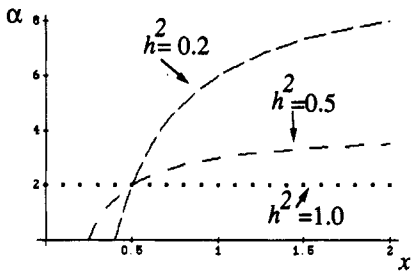


**Figure 12.** Plot of the critical field needed to produce tilting, $\alpha_c$, vs $x$ for various compressions. For $h^2 = 1$ there is no compression and the critical field is the same as for the Frederiks transition, i.e., $\alpha_c \approx 2$. At larger compressions ($h^2 < 1$) the critical field is lowered for small $x$ and is zero for even smaller $x$. However, for $x > 1/2$ the critical field increases with increasing compression.

molecular weight nematics one finds

$$\mathcal{B}_c \sim H^{-1} \tag{60}$$

The critical field increases when the layer is made thinner because the distortion penalty is heavier. Essentially the same behavior is expected from LCP in nematic solvents providing $h > 1$. Qualitatively different behavior is expected from confined layers, $h < 1$. Clearly no field is necessary in the region of confinement-induced tilt

$$\alpha_c = 0 \qquad x \le (1 - h^2)/2 \tag{61}$$

Outside the boundary of this region we have (Figure 12)

$$\alpha_c = \frac{2}{h^2} + \frac{1}{x}\left(1 - \frac{1}{h^2}\right) \qquad x > (1 - h^2)/2 \tag{62}$$

In the immediate vicinity of the critical confinement, $x_c = (1 - h^2)/2$, very small fields can trigger the tilting transition

$$\alpha_c = 2(x - x_c)/h^2 x \tag{63}$$

In this regime the critical field can be made arbitrarily small irrespective of its $h$ dependence. Note that for $x < 1/2$ the confinement assists the magnetic field and the critical field is thus lowered. The opposite trend is found for $x > 1/2$, where the compression makes tilt more difficult. In this last case the critical field increases with the compression.

## VI. Antagonistic Field

In the previous section we studied the case of a field which assists tilting. In the present section we will consider the case of an "antagonistic" field which opposes tilt. In our chosen system, tilting is penalized by a magnetic field oriented with the normal to the layer. The resulting behavior exhibits some interesting features. The appropriate Landau free energy is obtained by replacing $\alpha$ in (56–58) by $-\alpha$, thus leading to

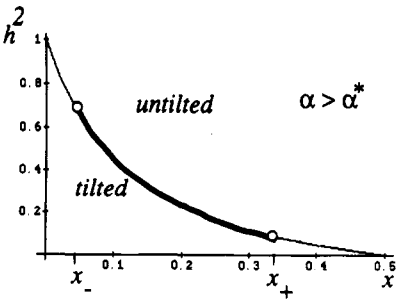


**Figure 13.** Phase diagram for the case of a weak antagonistic field, $\alpha < \alpha^*$. The tilting transition is second order, and only compressed systems are tilted.

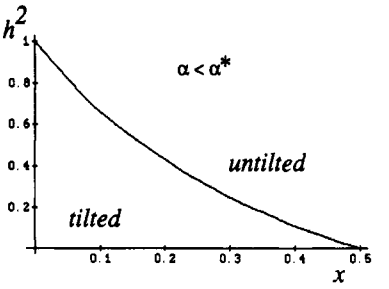


**Figure 14.** Phase diagram for the case of a strong antagonistic field, $\alpha > \alpha^*$. The distinctive features are the presence of a first-order "window" (solid line) in the critical line and the creation of two tricritical points (○). Only compressed configurations are tilted.

$$A = \frac{1}{x}[h^2(1 + \alpha x) - (1 - 2x)] \tag{64}$$

$$B = \frac{1}{8x}[1 + 3h^2 - 4x\alpha h^2] \tag{65}$$

$$C = \frac{1}{96x}[1 + 14h^2 + 8x\alpha h^2] \tag{66}$$

As a result, $B$ can change sign and a first-order transition may thus occur for large enough fields. Provided $\alpha < \alpha^* = (46 + 16(7^{1/2}))/9 \approx 9.8$ the transition is second order and the condition $A = 0$ yields (Figure 13)

$$h_c^2 = (1 - 2x)/(1 + \alpha x) \tag{67}$$

As expected, $h^2$ is lower in the presence of the field: Stronger confinement is needed to induce a tilt. For $\alpha > \alpha^*$ (Figure 14), a line of first-order phase transitions occurs in the interval

$$x_- \equiv \frac{1}{16\alpha}[3\alpha + 6 - (9\alpha^2 + 36\alpha - 92\alpha)^{1/2}] < x < x_+ \equiv \frac{1}{16\alpha}[3\alpha + 6 + (9\alpha^2 + 36\alpha - 92\alpha)^{1/2}] \tag{68}$$

No phase transition occurs if $x > 0.5$, and a second-order transition is expected if $x$ is outside the range in (68). There are thus two tricritical points at $x_-$ and $x_+$. The first-order line is specified by the solution of $B = -4(AC/3)^{1/2}$; however, the numerical results differ only slightly from those of (67). Accordingly, (67) can serve as a good approximation to the phase boundary for both the first- and second-order transitions.

Another property of interest is the critical field to *suppress* tilt. Clearly, no field is necessary for the unconfined layer, i.e., $\alpha_c = 0$ for $h > 1$. Also, no field is required outside the boundary of the region of confinement-induced tilt.

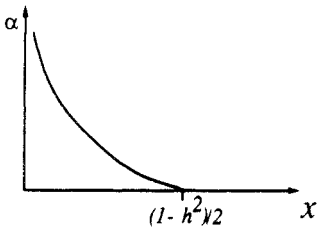


**Figure 15.** Plot of the critical antagonistic field needed to *suppress* tilt (see eq 69) for $h < 1$. For $x > {}^1/_2(1 - h^2)$ no field is needed to suppress tilt, but for small $x$ and large compressions the critical field increases as $x^{-1}h^{-2}$.

$$\alpha_c = 0 \quad h < 1 \quad \text{and}$$

$$x > {}^1/_2(1 - h^2)$$

Within this region the critical field is (Figure 15)

$$\alpha_c = (1 - 2x)/(h^2x) - 1/x \quad h < 1 \quad \text{and}$$

$$x > {}^1/_2(1 - h^2) \tag{69}$$

Since the field opposes tilt and the compression favors tilt (for $x < 0.5$), there are situations in which *removal* of the field causes tilt. One chooses $h$ and $x$ in the shaded region shown in Figure 16, i.e., between the transition lines in the presence and in the absence of antagonistic field. When the field is applied, the system is in an untilted state. Upon its removal it reverts to the "natural", tilted state.

## VII. Discussion

The mean field analysis presented above ignores many possible complications due to fluctuations, defects, and smectic order induced by the surface. Within this framework it is suggested that the behaviors of free LCPs in a melt and in a nematic solvent are qualitiatively similar. The two systems are expected to differ in their behaviors when interfaces become important. The distinctions arise because it is possible to orient the nematic solvent at the interface and, independently, to deform the LCP. Our discussion is concerned with a particular case: nematic solutions of LCPs in a narrow slit. However, related effects are expected in other systems such as layers of terminally anchored, grafted LCPs. Since these effects depend crucially on the solubility of LCPs in nematics of low molecular weight, it is useful to summarize the situation in this respect. The solubility of LCP in nematic solvents is well established experimentally.[3] The rule of thumb is that an LCP is soluble in a chemically similar nematic.[2] The theoretical analysis is less developed. A useful phenomenological approach was suggested by Brochard.[19] The familiar $\chi$ parameter is replaced by $\chi_n = \chi_0 + \chi_1 S^2$. $\chi_0$ describes the monomer–solvent interaction in the isotropic phase. A phenomenological correction for the effect of the nematic order is provided by the second term. For typical polymers, which are immiscible in nematic solvents, $\chi_1 \approx 1$. However, $\chi_1 \ll 1$ is expected for LCP in a chemically similar nematic solvent. Our discussion is concerned with the case of Θ nematic solvents, i.e., $\chi_n = {}^1/_2$. Since we are concerned with strongly ordered nematics, $S \approx 1$, this implies $\chi_0 < {}^1/_2$ and $\chi_1 < {}^1/_2$; that is, the nematic must be a good solvent in its isotropic state. However, we should stress again that the predicted effects are expected to take place, with certain modifications, in good solvents as well as in Θ solvents.

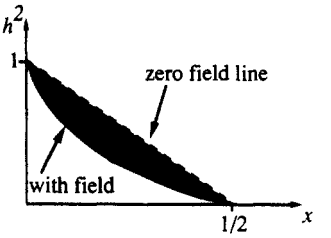


**Figure 16.** Phase diagram showing the region where the antagonistic field can be used as a switch. The broken line is the transition line in the absence of a field. Below this line the system is tilted when there is no field. The full line depicts the phase boundary in the presence of an antagonistic field. Above this line the system is untilted when the field is switched on. By arranging the system to lie in the shaded region the tilt can be switched off by the application of a field.

The confinement behavior considered can be studied in "mica machines" using solutions of LCPs in nematic solvents. The escape of LCPs from confinement should not pose a problem since the tilting transition is expected to take place at a much faster rate. Furthermore, rapid detection of the transition is possible because of the associated change in the birefringence of the sample. A related experiment, on pure low molecular weight nematics, was reported by Horn et al.[20] The incorporation of electric fields into mica machines was explored in different contexts.[21]

**Acknowledgment.** D.R.M.W. and A.H. enjoyed financial support provided by DOE Grant DE-FG03-87ER45288 and the Ford Motor Co. We thank G. Picket, T. Odijk, J. Israelachvili, H. W. Schmidt, and P. Pincus for helpful discussions.

## Appendix: Exact Analysis of the Transition

Here we show that the trial function (35), used for the case of compression in the absence of a field, is essentially exact near the second-order tilting transition. The method relies on the fact that (i) the actual director distortion, $\theta(z)$, corresponds to a free-energy minimum and (ii) the director distortion is small at the transition. The free energy can be written

$$\Gamma \int_0^H dz \left(\frac{d\theta}{dz}\right)^2 + M[(R_\parallel/\rho)^2 + \ln((\rho/R_\parallel)^2)] \tag{70}$$

where $\Gamma = (1 - \phi)K/2$, $M = kTH\phi/\alpha^2 L$, and $\rho$ is the arc-length distance between the plates, given by (34). Before the transition, $\theta(z) = 0$ everywhere. Since the transition is second order, $\theta(z)$ at the transition is small. We thus expand the free energy with respect to $\theta(z)$. The compression term is

$$M[(R_\parallel/H)^2 - 2\ln(R_\parallel/H)] + M(1 - (R_\parallel/H)^2)\frac{1}{H}\int_0^H dz\theta^2(z) \tag{71}$$

The nematic distortion term can be written by integrating by parts once, as

$$\Gamma \int_0^H dz \left(\frac{d\theta}{dz}\right)^2 = \Gamma\left[\theta(z)\frac{d\theta(z)}{dz}\right]_0^H - \Gamma \int_0^H dz\theta\frac{d^2\theta}{dz^2} \tag{72}$$

The first term vanishes by virtue of the boundary conditions $\theta(0) = \theta(H) = 0$. Combining the polymer and the bulk term gives a contribution independent of $\theta(z)$, which is of no interest, and a term in $\theta^2(z)$, of the form

$$\int_0^H dz\theta\left[ -\Gamma\frac{d^2\theta}{dz^2} + \frac{M}{H}(1 - (R_\parallel/H)^2)\theta\right] \quad (73)$$

This term must vanish for the minimal free energy, and the term in brackets is thus zero. $\theta(z)$ then satisfies the simple harmonic oscillator equation, subject to $\theta(0) = \theta(H) = 0$. The distortion is therefore $\theta(z) = Q\sin(\pi(2p + 1)z/H)$ at the transition, where $p$ is an integer. $p = 0$ yields the lowest energy, and thus the correct behavior of the distortion is $\theta(z) = Q\sin(\pi z/H)$.

## References and Notes


(1) Ciferri, A., Ed. *Liquid Crystallinity in Polymers*; VCH Publishers: Cambridge, U.K., 1991.
(2) Ringsdorf, H.; Schmidt, H.-W.; Schneller, A. *Makromol. Chem., Rapid Commun.* **1982**, *3*, 745.
(3) (a) Volino, F.; Gauthier, M. M.; Giroud-Godquin, A. M.; Blumstein, R. B. *Macromolecules* **1985**, *18*, 2620. (b) Volino, F.; Blumstein, R. B. *Mol. Cryst. Liq. Cryst.* **1984**, *147*, 113. (c) D'Allest, J. F., et al. *Phys. Rev. Lett.* **1988**, *61*, 2562.
(4) Williams, D. R. M.; Halperin, A. *Europhys. Lett.* **1992**, *19*, 693.
(5) Daoud, M.; de Gennes, P.-G. *J. Phys. (Paris)* **1976**, *38*, 85.
(6) Turban, L. *J. Phys. (Paris)* **1984**, *45*, 347.
(7) Halperin, A.; Alexander, S. *Macromolecules* **1987**, *20*, 1146.
(8) Brochard-Wyart, F.; Raphael, E. *Macromolecules* **1990**, *23*, 2276.
(9) Whittington, S. G.; Soteros, C. E. *Isr. J. Chem.* **1991**, *31*, 127.
(10) (a) de Gennes, P.-G. *The Physics of Liquid Crystals*; Clarendon: Oxford, U.K., 1974. (b) Chandrasekhar, S. *Liquid Crystals*; Cambridge University Press: Cambridge, U.K., 1977. (c) Vertogen, G.; de Jeu, W. H. *Thermotropic Liquid Crystals, Fundamentals*; Springer Verlag: Berlin, 1988.
(11) (a) de Gennes, P.-G. In *Polymer Liquid Crystals*; Ciferri, A., Krigbaum, W. R., Meyer, R., Eds.; Academic Press: New York, 1982. (b) Gunn, J. M. F.; Warner, M. *Phys. Rev. Lett.* **1987**, *58*, 393. (c) Warner, M.; Gunn, J. M. F.; Baumgartner, A. B. *J. Phys. A: Math. Gen.* **1985**, *18*, 3007. (d) Williams, D. R. M.; Warner, M. *J. Phys. (Paris)* **1990**, *51*, 317. (e) Williams, D. R. M.; Warner, M. In *Computer Simulation of Polymers*; Roe, R. J., Ed.; Prentice Hall: Englewood Cliffs, NJ, 1991. (f) Le Doussal P.; Nelson, R. *Europhys. Lett.* **1991**, *15*, 161. (g) Croxton, C. A. *Macromolecules* **1991**, *24*, 537. (h) Toner, J. *Phys. Rev. Lett.* **1992**, *68*, 1331. (i) Williams, D. R. M. *J. Phys. A* **1991**, *24*, 4427. (j) Selinger, J. V.; Bruinsma, R. F. *J. Phys. (Paris)* **1992**, *2*, 1215. (k) Warner, M.; Williams, D. R. M. *J. Phys. (Paris)* **1992**, *2*, 471. (l) Warner, M.; Gelling, K. P.; Vilgis, T. A. *J. Chem. Phys.* **1988**, *88*, 4008. (m) Kamien, R. D.; Le Doussal, P.; Nelson, D. R. *Phys. Rev. A* **1992**, *45*, 87227.
(12) Jerom, B. *Rep. Prog. Phys.* **1991**, *54*, 391.
(13) Odijk, T. *Macromolecules* **1986**, *19*, 2313.
(14) For a review, see: Khokhlov, A. R.; Semenov, A. N. *Sov. Phys. Usp.* **1988**, *31*, 988.
(15) Vroege, G. J.; Odijk, T. *Macromolecules* **1988**, *21*, 2848.
(16) Khokhlov, A. R.; Semenov, A. N. *J. Phys. A: Math. Gen.* **1982**, *15*, 1361.
(17) For a recent discussion, see: Birshtein, T. M.; Pryamitsin, V. A. *Macromolecules* **1991**, *24*, 1554.
(18) Huang, K. *Statistical Mechanics*; Wiley: New York, 1987.
(19) Brochard, F. *J. Phys. (Paris)* **1979**, *40*, 1049.
(20) Horn, R. G.; Israelachvili, J. N.; Perez, F. *J. Phys. (Paris)* **1981**, *42*, 39.
(21) (a) Fan, R. F.; Bard, A. J. *J. Am. Chem. Soc.* **1987**, 109. (b) Smith, C. P.; Maeda, M.; Atanasoska, L.; White, H. W.; McClure, D. J. *J. Chem. Phys.* **1988**, 92. (c) Horn, R. G.; Smith, D. T. *Science* **1991**, *256*, 362.